Advances in Cancer Biology - Metastasis 4 (2022) 100045

Contents lists available at ScienceDirect

Advances in Cancer Biology - Metastasis

journal homepage: www.journals.elsevier.com/advances-in-cancer-biology-metastasis

Glioblastoma cell invasiveness and epithelial-to-mesenchymal transitioning are modulated by kinin receptors

Mona N. Oliveira [a,e,f], Micheli M. Pillat [a,b], Juliana Baranova [a], Roberta Andrejew [a], Balbino Lino dos Santos [c], Silvia Lima Costa [c,d], Tamara T. Lah [e,f,**], Henning Ulrich [a,*]

[a] Department of Biochemistry, Institute of Chemistry, University of São Paulo, Av. Prof. Lineu Prestes 748, São Paulo, SP, 05508-000, Brazil
[b] Department of Microbiology and Parasitology, Health Sciences Center, Federal University of Santa Maria. Av Roraima 1000, Santa Maria, RS, 97110-970, Brazil
[c] Laboratory of Neurochemistry and Cell Biology, Department of Biochemistry and Biophysics, Institute of Health Sciences, Federal University of Bahia, 40110-902, Salvador, Bahia, Brazil
[d] National Institute for Translational Neuroscience (INCT/CNPq INNT), Institute of Biomedical Science /UFRJ, Av. Carlos Chagas Filho 373, CEP 21941-902, Rio de Janeiro, Brazil
[e] Department of Genetic Toxicology and Cancer Biology, National Institute of Biology, Večna pot 111, 1000, Ljubljana, Slovenia
[f] Jožef Stefan International Postgraduate School, Jamova cesta 39, 1000, Ljubljana, Slovenia

ARTICLE INFO

Keywords:
Cell fusion
Glioblastoma
Invasion
Kinin signaling
Mesenchymal stem cells
Tumor microenvironment

ABSTRACT

Glioblastoma (GB) is the most aggressive primary tumor of central nervous system, where no efficient therapy has been found so far. This is due to high intra- and inter- tumor heterogeneity, fast invasion and the therapy-resistant subpopulation of GB stem cells and their plasticity. Tumor heterogeneity involves interactions among cancer cells and stromal cells, such as mesenchymal stem cells (MSCs), that are recruited into the tumor microenvironment and migrate to the tumor site. Here, we characterized the impact of kinin receptors on the interaction of MSCs with GB cells which is further enhanced by kinin receptor agonists. Interactions between GB cells and MSCs were studied in two- and three-dimensional co-cultures. Kinin receptor activity was modulated by selective agonists and antagonists to evaluate their influence on cell viability, cell-cell interactions, GB U87 cell invasiveness, and phenotype alterations. Tumor cell invasion was enhanced by the kinin-B2 receptor agonist bradykinin, while it was blocked by B2 receptor antagonists applied in U87 cells monoculture and in co-culture with MSCs. Kinin receptor inhibition correlated with enhanced direct U87/MSC interactions, such as heterotypic fusion, vesicle transfer and entosis. Furthermore, kinin receptor modulation influenced expression of F-actin expression and genes associated with epithelial-to-mesenchymal transition in U87 cells upon U87/MSCs co-cultures. Our data support ongoing investigations of kinin receptor inhibition as an adjuvant approach in GB therapy. MSC impacts on cancer progression need further investigation, as they may have a synergistic effect with kininergic receptor activation.

1. Introduction

Glioblastoma (GB), recently classified as a "diffuse glioma with no mutations in IDH genes WHO grade IV" is the most aggressive form of glioma (World Health Organization grade IV and updated by European Association of Neuro-Oncology) [1,2]. Its rapid progression and aggressiveness arise partially from cooperative interactions among genetically distinct malignant subclones of GB cells, including the small population of GB stem cells (GSCs). Based on gene expression patterns, somatic mutations and DNA copy numbers, the GB subtypes are now clustered into three major subpopulations: proneural (PN), classical (CL) and mesenchymal (MES), which are guided by three key oncogenes, such as platelet growth factor receptor-α (*PDGFRA*) activation, epidermal growth factor receptor (EGFR) activation, and tumor suppressor neurofibromin 1 (*NF1*) deletions, respectively. The phenotype and prognosis of GB subtypes differ. Patients with MES type have the shortest overall survival, whereas the median survival of patients with

* Corresponding author. Department of Biochemistry, Institute of Chemistry, University of São Paulo, Av. Prof. Lineu Prestes 748, São Paulo, SP, 05508-000, Brazil.
** Corresponding author. Department of Genetic Toxicology and Cancer Biology, National Institute of Biology, Večna pot 111, / Jožef Stefan International Postgraduate School, Jamova cesta 39, 1000, Ljubljana, Slovenia.
E-mail addresses: mona@biolinker.tech (M.N. Oliveira), micheli.pillat@ufsm.br (M.M. Pillat), jbaranova@usp.br (J. Baranova), roberta.andrejew@gmail.com (R. Andrejew), balbinolino26@gmail.com (B.L. dos Santos), costasl@ufba.br (S.L. Costa), tamara.lah@nib.si (T.T. Lah), henning@iq.usp.br (H. Ulrich).

https://doi.org/10.1016/j.adcanc.2022.100045
Received 28 February 2022; Received in revised form 10 May 2022; Accepted 11 May 2022
Available online 19 May 2022

List of abbreviations

Akt	Protein kinase B
B1R	Kinin B1 receptor
B2R	Kinin B2 receptor
BK	Bradykinin
BM-MSCs	Bone marrow-derived mesenchymal stem cells
CD	Cluster of differentiation
CL	Classical glioblastoma subtype
DBK	Des-Arg^9-bradykinin
DMEM	Dulbecco's modified Eagle's medium
DsRed	Discosomal red fluorescent protein
eGFP	Enhanced green fluorescent protein
EMT	Epithelial-to-mesenchymal transition
ERK1/2	Extracellular signal-regulated kinase 1/2
FBS	Fetal bovine serum
GB	Glioblastoma
GSCs	Glioblastoma stem cells
HEPES	4-(2-hydroxyethyl)-1-piperazineethanesulfonic acid
HOE-140	D-Arg-L-Arg-L-Pro-L-Hyp-Gly-L-(2-thienyl)Ala-L-Ser-D-1,2,3,4-tetrahydro-3-isoquinolinecarbonyl-L-(2α,3β,7aβ)-octahydro-1H-indole-2-carbonyl-L-Arg
IL-8	Interleukin 8
MES	Mesenchymal glioblastoma subtype
MMP	Metalloproteases
MSC(s)	Mesenchymal stem cell(s)
MTS	3-(4,5-dimethylthiazol-2-yl)-5-(3-carboxymethoxyphenyl)-2-(4-sulfophenyl)-2H-tetrazolium
MTT	3-(4,5-dimethylthiazol-2-yl)-2,5-diphenyltetrazolium bromide
NF-κB	factor nuclear kappa B
PBS	Phosphate buffered saline
PCR	Polymerase chain reaction
PI3K	Phosphoinositide 3-kinase
PN	Proneural glioblastoma subtype
R715	AcLys[D beta Nal7, Ile8] desArg^9-bradykinin
Snail	Zinc finger protein SNAI1
STAT3	Signal transducers and activators of transcription 3
TGF-β	Transforming growth factor-beta
TME	Tumor microenvironment
WHO	World Health Organization
ZEB	Zinc finger E-box-binding homeobox

PN type is the longest [3,4]. Regarding GB cell lineages, U373 (or U251) cells best represent the MES type, whereas the U87 lineage has more PN characteristics [5]. Zarkoob and coworkers were the first to suggest that there is a link between molecular subtypes of GB and epithelial-to-mesenchymal transition (EMT) transition, which enables the transition among different subtypes [5,6]. EMT is a principal inductor for the change of tumor microenvironment (TME), triggered by enhanced expression of E−cadherin and vimentin, reorganization of cytoskeleton polarity and signaling transduction cues mediated by transforming growth factor (TGF)-β and factor nuclear kappa B (NF-κB), as well as by the pro-inflammatory transcription factor Snail. The principal markers for EMT are TGF-β, vimentin and Snail, which have augmented expression [7] and result in pro-inflammatory events and tumor invasiveness.

There are numerous heterotyping interactions among tumor and stromal cells in the TME [8]. In GB, tumor-resident astrocytes and microglia, besides neural cells, endothelial cells, immune cells and mesenchymal stem cells (MSCs) are part of the TME, affecting GB cells and getting affected by them in return. Bone-marrow-derived mesenchymal stem cells (BM- MSC) [9–12] and MSCs have a unique role in TME, since they can transdifferentiate into tumor-associated fibroblasts, pericytes, and potentially even GSCs [13]. Schichor and collaborators (2012) [14] speculated that MSCs and GB cells interact directly *via* gap junctions and may form the functional syncytium. These structures would promote cell fusion, where U87 cells may acquire a MES phenotype when co-cultured with MSCs, as reflected by the increased expression of MSC-associated markers such as CD29, CD90, and CD105 [15]. CD105 is an accessory protein of the TGF-β receptor family expressed by brain tumors of a higher grade [16]. MSCs also induce the transformation of cancer cells into MES phenotypes, such as shown for colon cancer cells [17]. Furthermore, Breznik et al. (2017) highlighted U87 and U373 cell line-specific responses to BM-MSCs during two- and three-dimensional direct co-culture: BM-MSCs inhibited the migration of U87 cells, while they enhanced the migration of U373 cells [5]. BM-MSC-induced U373 cell migration is assisted by overexpression of various proteases, which are mediators of interactions between cancer and stromal cells [5]. On the other hand, Motaln et al. showed that MSCs are responsible for the impairment of U87 cell invasion and growth [18].

An important feature of MSCs is the modulation of the immune response that in addition to cytokines involve the exchange of extracellular vesicles [18–21]. MSCs have been attributed to therapeutic capacities in tissue and brain repair. They have been shown to transdifferentiate into distinct neural phenotypes [22] and to improve neurological conditions, as recently reported in a study using a transgenic Alzheimer's mouse model [23]. Among the pro-inflammatory mediators, kinins play a special role in the TME. The endogenous kallikrein-related proteolytic cascade, starting from plasma or tissue kininogens, results in the release of bioactive kinins, such as kallidin and bradykinin (BK). Kinins are involved in various physiological conditions, including neurogenic differentiation [24,25], and pathophysiological processes, such as tumorigenesis [26] and glioma progression [27–29]. Kinins act through two G-protein coupled receptors: kinin B1 (B1R) and B2 (B2R) receptors, which convey different pharmacological effects. The B2R is activated by BK and kallidin, obtained by cleavage of low and high molecular weight kininogens. B1R activates in the presence of metabolites of BK and kallidin (des-Arg^9-bradykinin (DBK) and des-Arg^{10}-kallidin, respectively) that originate from kinin cleavage at the C-terminus by type I kinases (carboxypeptidases) [30,31]. In contrast to the B2R, which is expressed in a wide variety of cells and tissues, the B1R is hardly expressed under normal conditions but can be induced by endotoxins, cytokines, and growth factors, indicating its specific role in pathological processes [32,33].

Various antagonists for both receptors have been tested in phase II clinical trials for prostate cancer treatment [34]. However, the effects of kinins are cancer-type specific and not always beneficial in tumor treatment: it has been observed that B1R activation suppresses the growth of melanoma cells [35], while promoting the proliferation of estrogen-sensitive breast cancer cells [36]. B1R and B2R antagonism or double knockout of the genes resulted in reduced tumor size and lower mitotic index in the GB mouse model injected with GL-261 cells [37].

B2R expression was decreased in low-grade and increases gradually in WHO grades III and IV in patients' biopsies [38], whereas high B1R expression was noted in low-grade gliomas in older patients with GB [37]. B1R expression is induced in GB by high levels of inflammatory cytokines, produced by tumor-infiltrating immune cells including MSCs [39]. As a part of a feedback loop, B1R activation induces interleukin (IL)-8 expression in GB cells, which leads to STAT3 activation and higher migratory capacity of cancer cells [40]. Pillat and colleagues (2016) have shown that both B1R and B2R are expressed in U87 cells and MSCs [41]. During indirect and direct U87/MSC co-cultures, B1R expression increased in U87 cells, correlating with enhanced invasiveness of cells *via* induction of metalloproteases (MMPs) [41]. Moreover, differential responses between U87 and U373 cells have also been noted: the B1R agonist, DBK, stimulated U87/MSC, but not U373/MSCs, spheroid formation and increased migration/invasion of U87 cells. It is feasible that such effect was related to a significantly reduced B1R expression in U373 cells [37,41].

Herein, we further investigated the role of kinin receptors, mainly of the B2R subtype, in U87 or U373 cells co-cultured with human BM-MSCs (herein abbreviated as MSCs) to study the mechanisms of GB cells invasion and confirm the previously suggested co-stimulatory effect of B1R and B2R. Obtained results imply that GB-MSC communication mediated by kininergic signaling impacts the GB cell invasion *via* EMT.

2. Materials and methods

2.1. Cell lines and culture maintenance

The human GB cell lines U87 [American Type Culture Collection (ATCC) number HTB-14] and U373 [ATCC HTB-17, reclassified as U251 cells] were obtained from ATCC and regularly authenticated, according to a previous study [42]. Cells were grown in Dulbecco's modified Eagle's medium (DMEM) supplemented with 10% fetal bovine serum (FBS), non-essential amino acids, 4 mM L-glutamine, 100 U/mL penicillin and 100 µg/mL streptomycin (Gibco). U373 cells were stably transfected with pEGFP-N1 (ClonTech) for enhanced green fluorescent protein (GFP) as described previously [14]. U87 cells expressing red fluorescent protein (DsRed) were prepared as described previously [41].

$U87^{DsRed}$ and $U373^{GFP}$ cells were routinely propagated culture medium containing 1 mg/mL geneticin (G-418, Sigma-Aldrich). GB cells were passaged after reaching 75% confluence and plated for culture maintenance at a density of 15,000 cells/cm^2. U87/$U87^{DsRed}$ cells of passages 40–58 were used for the experiments.

Human BM-MSCs derived from a healthy volunteer (clone MSC-2) were purchased from Lonza Bioscience Walkersville (Walkersville, MD). After resuspension, cells were plated and grown in the same medium as the GB cells. MSCs of passages 8–12 were used for the experiments and they were passaged after reaching 75% confluence at a density of 7,000 cells/cm^2. All cells were cultured at 37 °C, in a humidified atmosphere supplied with 5% CO_2. Medium changes were performed every three days.

2.2. Two-dimensional (2D) and three-dimensional (3D) cell cultures

For 2D direct mixed cells co-culture, GB cells and MSCs in various combinations (U87/MSCs, $U87^{DsRed}$/MSCs, U373/MSCs, and $U373^{GFP}$/MSCs) were plated in the 6-well plates at 1:1 ratio and cultured for 1–7 days. For the preparation of the 3D/spheroid cultures, the cells were distributed into 96-well U-bottomed plates (2.5×10^3 cells/well; Corning, Life Sciences, MA) in 200 µL complete DMEM growth medium containing 4% methylcellulose. For the mixed spheroids, a 1:1 ratio of MSCs to GB cells was used. The cells were centrifuged for 90 min at $850 \times g$ and left for 1 day in the incubator to form the spheroids.

2.3. MTT assay after culture treatment with agonists and antagonists

The B2R agonist BK, and its selective antagonist, HOE-140, as well as the selective B1R antagonist, AcLys[D beta Nal^7, Ile^8]desArg^9-bradykinin (R715) (Tocris, Fisher Scientific, Pittsburg, PA), were added to the growth medium or into the matrigel of the spheroids at final concentrations of 1–100 nM. The spheroids were grown in the presence of drugs for 1–7 days in 96-well plates in FBS-free medium. For the MTT assay, the medium was exchanged for a new one containing 20 µl of MTT reagent following incubation for 4 h at 37 °C. The formazan crystals were dissolved in high-purity isopropanol, and absorbances were read at 540 nm using a microplate reader (Genios; Tecan, Bradenton, FL). The measurements were performed in triplicates and experiments were repeated three times.

2.4. MTS assay in spheroid cultures

After the spheres were formed (1-day post-seeding), the FBS-free medium (200 µL/per well of the 96-well plate) was supplemented with the kinin receptor activity modulators (100 nM). Cell metabolic activity within the spheroids was determined using the MTS assay. After 1, 3, and 5 days, treated and control spheroids were submerged in 100 µL medium containing 20 µL MTS reagent (Promega). The spheroids were incubated for 3 h at 37 °C and assayed at 490/630 nm fluorescence excitation/emission using a microplate reader (Genios; Tecan, Bradenton, FL). The measurements were performed in triplicate and experiments were repeated three times.

2.5. MSC labelling and $U87^{DsRed}$ cell selection for MSC/U87 cell interaction studies

MSCs were pre-loaded with DiO green and kept in monoculture or co-culture with $U87^{DsRed}$ cells for 8 days, with medium changes every 2 days. Control culture of $U87^{DsRed}$ and MSCs were kept in parallel. On the third day, the medium was supplemented with geneticin (2 mg/mL) to select the $U87^{DsRed}$ cells containing the neomycin resistance gene. On the eighth day, the surviving cells in $U87^{DsRed}$ monoculture and U87/MSCs co-culture were collected for the mRNA extraction using with Trizol-chloroform method.

2.6. Live cell imaging

Images of untreated and treated cells with B2R and B1R antagonists (100 nM) living cells were recorded after 24, 48, 72, 96 and 168 h using an inverted microscope (Nikon Instruments, Melville, NY) coupled to a digital camera. The micrograph images were processed using the NIS-Elements 2.3v software for measuring the areas and cell distances, and for merging the fluorescent signals ($U87^{DsRed}$ and MSCs loaded with DiO green). Five micrograph images were taken per experimental condition. For the time-lapse imaging, the cells were pre-loaded with the respective dye as already described [15]. Cells were plated in 25 cm^3 T-flasks and co-cultured for 48h in the absence or presence of kinin receptor modulators. Prior to imaging, the medium was supplemented with 5 mM HEPES. Automated focus was applied and the loop time was set at 7 min for 12 h.

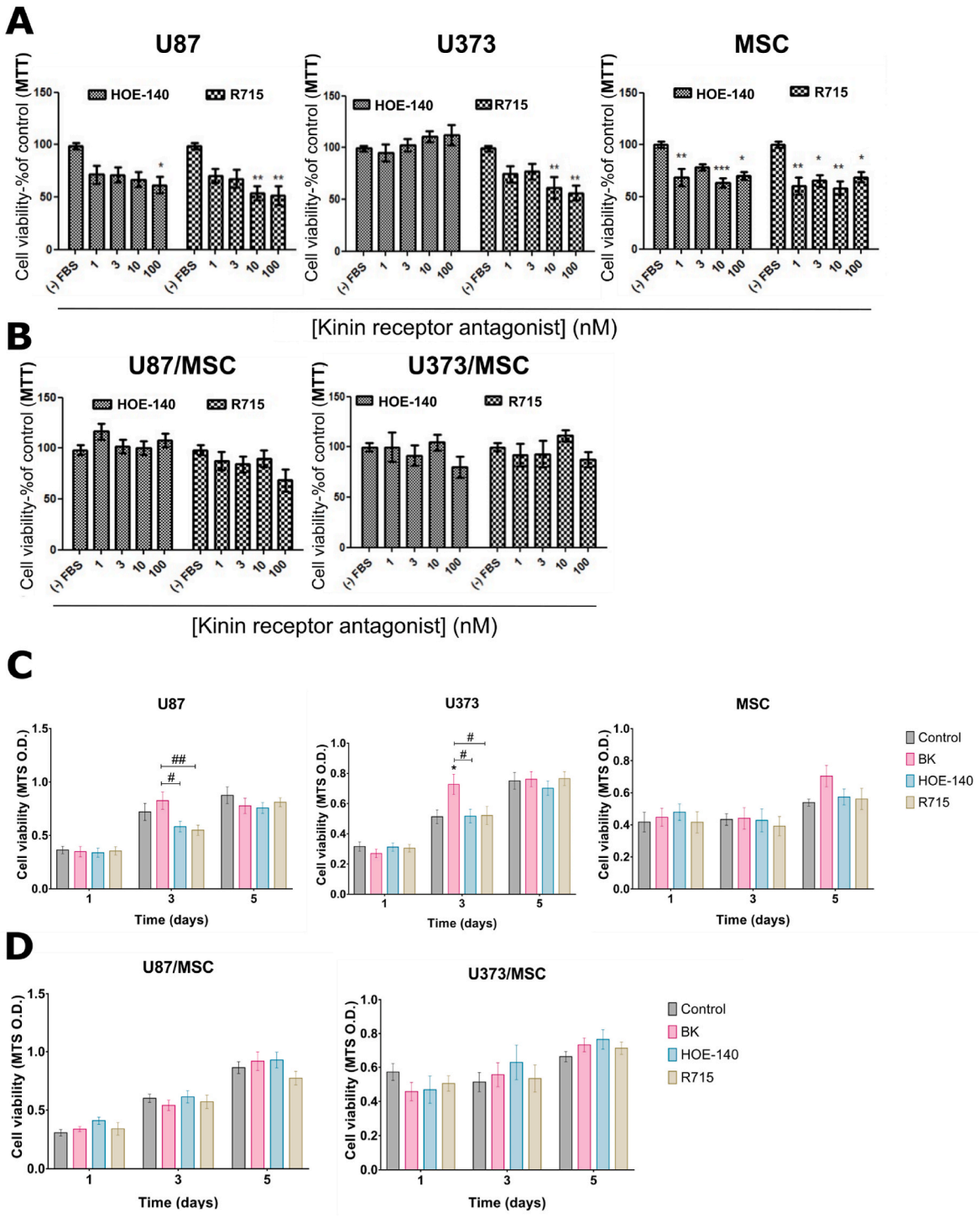

Fig. 1. Effects of kinin receptor antagonists and agonists on cell viability.
Metabolic cell activity of **(A)** U87, U373 and MSCs cells in 2D monoculture and (**B**) U87/MSC and U373/MSC in 2D co-culture was determined by the MTT assay 72 h after the treatment with the B2R antagonist HOE-140 or the B1R antagonist R715 at 1 nM, 3 nM, 10 nM, and 100 nM concentrations in the absence of FBS. One-way ANOVA followed by Bonferroni's multiple comparison test detected differences in 100 nM HOE-140 and 10 and 100 nM R715 in U87 monoculture; in 10 and 100 nM R715 in U373 monoculture; and 1, 10 and 100 nM HOE-140 and 1, 3, 10 and 100 nM R715 in MSC monoculture. *p<0.05; **p<0.01. Metabolic cell activity of (**C**) U87, U373, and MSCs in spheroid monoculture and **(D)** U87/MSC and U373/MSC spheroid co-culture after treatment with BK (100 nM), HOE-140 (100 nM) or R715 (100 nM) for 1, 3 and 5 days was determined by the MTS assay. Two-way ANOVA followed by Bonferroni's multiple comparison test showed differences in BK treatment on day 3 in U87 and U373 spheroids monoculture (U87: # BK vs. HOE-140, p = 0.0253; and ## BK vs. R715, p = 0.0073, respectively. U373: * BK vs. control, p = 0.0147; # BK vs. HOE-140 and R715, p = 0.0147 and 0.0170, respectively). Data are presented as mean ± SEM and are representative of three independent experiments. BK: Bradykinin.

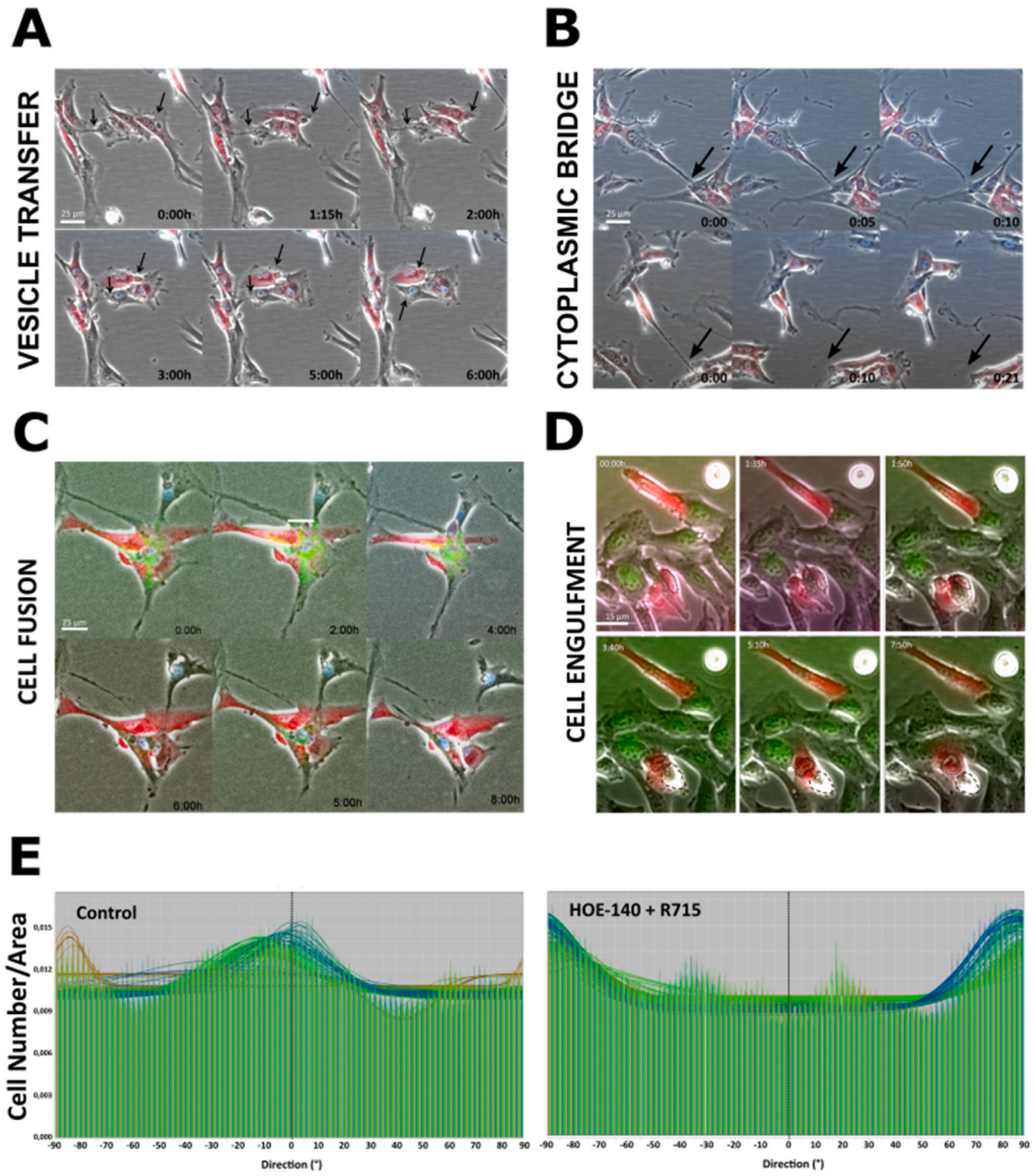

Fig. 2. Cell-cell interactions and cell motility in U87/MSC co-culture.
(**A**) Hourly obtained time-lapse microscopy images (0–6 h) of U87^{DsRed} cells (red) and MSCs (non-labeled) following 3 days of co-culture. Arrows point to the vesicles being transferred between the cells. Scale bar = 25 μm. **(B)** Visualization of cytoplasmic bridges formed between U87^{DsRed} (red) cells and MSCs (non-labeled) pointed by the arrows. The time presented in the image is relative to the Supplementary Video 1 timing. Scale bar = 25 μm. (**C**) Time-lapse microscopy images showing the cell fusion process between U87^{DsRed} (red) and MSCs (labeled with DiO green) pre-cultured for 3 days and then in the presence of HOE-140 and R715 (100 nM, respectively) for 8 h. Scale bar = 25 μm. (**D**) Time-lapse imaging of U87^{DsRed} (red) cells and MSC (labeled with DiO green) pre-cultured for 3 days and then cultured in the presence of HOE-140 and R715 (100 nM, respectively) for 8 h. Nuclear tracking was monitored to confirm entosis (dotted line). The nucleus acquired a moon-like shape during cell internalization (solid perimeter indicates the U87 cell nucleus and dashed line highlights the MSC nucleus). Scale bar = 15 μm. (**E**) Cell directionality histograms representing cell motility in the co-culture conditions in the absence or presence of HOE-140 plus R715 treatments, in the defined area, measured as described in the 2.7 methods' section. Local gradient analysis was used to calculate the number of cells in a certain direction (angulations, °), using Fiji. 3.0 software. The points were monitored along the time scale, and the plot presents the cell number in known angulations and the angulations variation over time. (For interpretation of the references to colour in this figure legend, the reader is referred to the Web version of this article.)

2.7. Directional cell movement analysis

U87 cells were treated with B2R and B1R antagonists (100 nM) and directionality was recorded for 12 h. The analysis of cell directionality was made using Fiji plugin from Image J to infer the preferred orientation of structures present in the input image. It computes a histogram indicating the amount of structures in a given direction. Images with completely isotropic content are expected to give a flat histogram, whereas images with a preferred orientation give a histogram with a peak at that orientation. The method used was the local gradient orientation. The local gradient of the image was calculated using a 5x5 Sobel filter, which is used to derive the local gradient orientation. This orientation was then used to build the histogram, by putting the square of the gradient norm in the adequate bin. The plugin used a fit by a Gaussian to compute directionality parameters, where the Gaussian fit has the following formula:

$$y = a + (b - a)^{*}\exp\left(- \frac{(x - c)^2}{2d^2} \right)$$

2.8. Immunofluorescence labeling

Monocultures of MSCs and U87^{DsRed} cells as well as co-cultures (at 1:1 ratio) were set up. Upon 72 h of culture, the cells were fixed with 4% paraformaldehyde in PBS for 15 min, washed three times with PBS, and incubated in a blocking solution containing 0.05% Triton-X 100 and 2% FBS for 30 min. Next, the cells were incubated for 30 min with Phalloidin-iFluor 488 Reagent, CytoPainter (ab176753; 1:100, Abcam, UK) which labels F-actin filaments. Samples were washed three times with PBS, followed by incubation for 15 min with Hoechst 333482 to stain nuclei. Following the washing step, slides were mounted with Vectashield mounting medium (Vector Laboratories, Burlingame, CA) and imaged using the Nikon epifluorescence microscope (Nikon Instruments, Melville, NY), equipped with a Nikon camera. Nikon image analysis software was used to analyze the images.

2.9. Flow cytometry

Different types of mixed cells (U87^{DsRed}/MSCs) were cultured for 3 days after treatment with BK, HOE-140, R715 or HOE-140 plus R715. U87 cells were selected from a co-culture using geneticin treatment for 6 days. The culture was dissociated, and single-cell suspensions were fixed with 4% paraformaldehyde for 20 min, washed with PBS supplemented with 1% FBS. Cells were incubated with anti-CD105 antibody conjugated with PerCP-Cy5.5 followed by incubation with Phalloidin conjugated with Alexa Fluor™ 647, for 30 min each at room temperature. Cells were washed with PBS and analyzed using the MACSQuant® Analyzer 10 Flow Cytometer (Miltenyi Biotech, Bergisch Gladbach, Germany). U87 cells and MSCs were discriminated based on Dio (FL1-H) and DsRed (FL2-H) fluorescence signals, following the compensation and elimination of non-specific signals. Experiments for quantification of CD105 and F-actin expression levels were performed as previously described [41]. A minimum of 10,000 events were counted per sample. The characterization of phenotypic markers was performed using a BD FACSCalibur™ Flow Cytometer (BD Biosciences, San Jose, CA). Data were displayed at logarithmic scales and analyzed with the FlowJo V10 software.

2.10. Three-dimensional invasion assay

The 3D invasion assay was performed as follows: the spheroids were covered with 5 mg/mL Matrigel (BD Bioscience, NJ) into 96-well U-bottomed plates. After a 45 min incubation at 37 °C, DMEM supplemented with 10% FBS was added in the presence, or absence (control group), of 100 nM BK or HOE-140. The initial area of the distance of invasion (T0) was measured following an overnight incubation, and then on seven successive days. The area of distance was measured from the edge of the spheroid by using the NIS elements software 2.3v (Nikon Instruments, Melville, NY) and normalized to the size of the spheroid.

2.11. Determination of EMT gene expression by real-time PCR

RNA was isolated using the Trizol reagent (Life Technologies) from 2D monolayer monoculture of U87 cells, mixed co-cultures (U87/MSCs) and U87 selected cells after treatment with BK, HOE-140 or HOE-140 plus R715. The cDNA was generated from 1.0 μg mRNA using the High-Capacity cDNA Reverse Transcription kit (Applied Biosystems, ThermoFisher, MA). The relative quantification of gene expression levels of B2R, Vimentin, CD44, Snail, TGF-β, and GADPH was carried out using real-time PCR (ABI 7900 HT Sequence Detection System; Applied Biosystems, ThermoFisher, Waltham, MA). These reactions were performed using 1:10 dilutions of each cDNA, TaqMan Universal PCR Master Mix and TaqMan Gene Expression Assays (Applied Biosystems, ThermoFisher, Waltham, MA): for B2R–Hs00176121_m1, Vimentin-Hs00185584_m1, CD44-Hs00174139_m1, Snail-Hs00195591_m1, Tgfb2-Hs00234244_m1 versus the amplification of GADPH (pre-developed TaqMan Assay Reagent No. 4310884E) as an internal control. The SDS v2.2 software (Applied Biosystems, ThermoFisher, Waltham, MA) was used to analyze the data obtained from the TaqMan Gene Expression Assays. The ΔΔCt method was used for relative quantification of gene expression.

3. Results

3.1. Effects of kinin receptor activity modulation on cell viability of GB cells and MSCs in mono- and co-cultures

Firstly, we performed a dose-response study to evaluate the effects of increasing doses (1 nM–100 nM) of the B2R antagonist (HOE-140) and the B1R antagonist (R715) on cell metabolism in monoculture and co-culture conditions using the MTT assay. HOE-140 treatment did not affect U373 cells and decreased U87 cell metabolism at the highest used concentration (100 nM), suggestive of decreased cell viability or cell toxicity (Fig. 1-A). The application of R715 significantly decreased the metabolism of both GB cell lines (up to 50%). Both kinin receptor antagonists decreased MSC metabolic activity (Fig. 1-A), whereas they did not affect activities of cells that had been co-cultured (Fig. 1-B).

After 3 days of culture with 100 nM BK, the MTS assay indicated a significant increase in metabolic activity in U373 spheroids monoculture when compared with U373 spheroid subjected to 100 nM HOE-140 or R715 treatments (Fig. 1-C). Similar results were observed in U87 spheroids monoculture after 3 days of 100 nM BK treatment relative to 100 nM R715 and HOE-140 treatments (Fig. 1-C). No significant effects on metabolic activity following 3 and 5 days were achieved by kinin receptor agonists/antagonists in MSC monoculture and GB-MSC co-cultures (Fig. 1-C, D).

Taken together these results show that viabilities of GB cells and

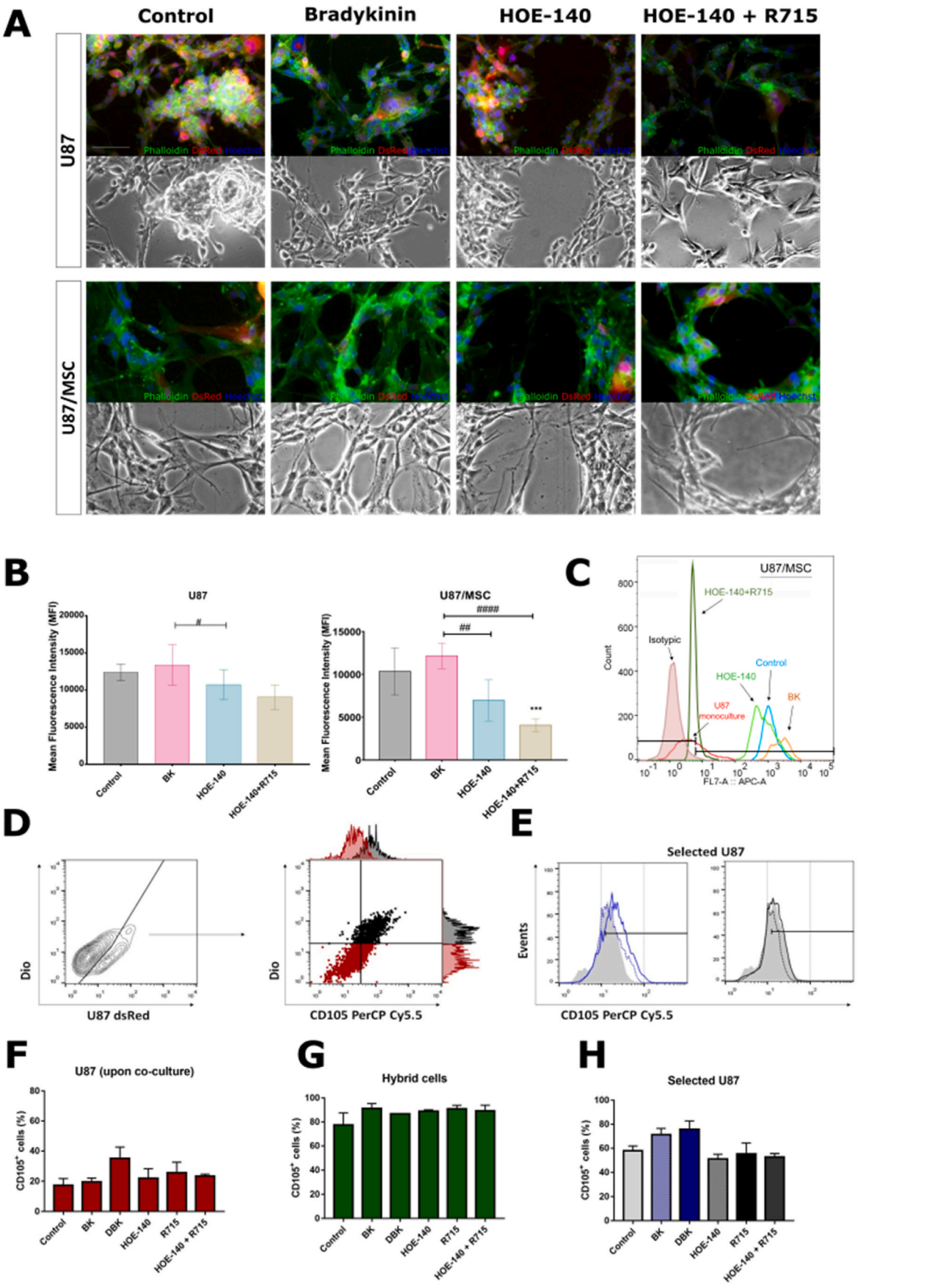

(caption on next page)

Fig. 3. Effects of kinin receptor agonism and antagonism on F-actin expression and EMT of U87 cells upon co-culturing with MSCs.
(**A**) Representative immunofluorescence images of U87^{DsRed} (red) monoculture and U87/MSC co-culture after 3 days in the absence or presence of 100 nM BK, HOE-140 or HOE-140 plus R715 treatments. F-actin staining (green, Phalloidin-iFluor 488). Nuclei were stained with Hoechst (blue). Scale bar = 100 μm. (**B**) Quantification of mean fluorescence intensity (MFI) of U87 cells and U87/MSC co-culture after treatment with BK, HOE-140 or HOE-140 plus R715 at 100 nM. In U87 cells, BK treatment slightly increased and HOE-140 decreased F-actin expression relative to BK ($p = 0.0193$). In U87/MSC co-culture, HOE-140 plus R715 treatment decreased F-actin expression relative to the control and BK groups ($p = 0.0009$ and $p < 0.0001$, respectively), whereas HOE-140 alone also decreased its expression relative to BK group ($p = 0.005$). The analysis was performed by flow cytometry and quantified with the FlowJo V10 software. Representative histograms are shown in **(C)**. Data are representative of three independent experiments and are shown as mean ± SD. **(D)** Effects of kinin receptor agonist and antagonist treatment were determined on EMT phenotype transition of U87 cells in monocultures and upon co-culturing with MSCs. Flow cytometry analysis did not reveal any differences in CD105 expression levels in mono- and co-cultures (MSCs loaded with DiO green, U87^{DsRed} and hybrid cells, DiO^{+}-DsRed^{+}) in the absence or presence of agonists or antagonists of kinin receptors (BK, DBK, HOE-140 and R715). **(E)** Flow cytometry histograms comparing the expression of CD105 in selected U87 cells without or with pharmacological activity modulation of B1R and B2R**.** Upper-left panel: Blue dotted line = BK; Blue line = DBK. Upper-right panel: Black dotted line = HOE-140; Black line = R715. Data were analyzed with Flowjo V10 software. **(F)** Percentages of CD105^{+} cells of U87 cells under co-culture condtition, **(G)** U87/MSC hybrids and **(H)** geneticin-selected U87 cells. Selection of U87^{DsRed} cells by geneticin treatment was performed for 6 days. Data are representatives of two independent experiments and are shown as mean ± SEM. BK: Bradykinin; DBK: des-Arg^{9}-bradykinin. (For interpretation of the references to color in this figure legend, the reader is referred to the Web version of this article.)

MSCs were sensitive to the presence of kinin receptor activity modulators and, in addition, this sensibility is quenched in GB-MSC co-cultures conditions.

3.2. Phenotypical changes and interactions between MSCs and U87 cells in co-culture

Our previous study demonstrated that U87 cells interact with MSCs more extensively than U373 do [15]. Upon co-culture, U87^{DsRed}/MSCs formed synkaryons, suggesting cell fusion or entosis [15]. Therefore, we used the U87/MSC co-culture for the current study. We used live cell imaging for a better understanding of the molecular events for the formation of cell hybrids. Vesicle transfer between MSCs and U87 cells was observed after 3–6 h of culture in both directions (Fig. 2-A, Supplementary Video 1) and cell-cell interactions (e.g. visible cytoplasmic bridges) were also observed in the co-cultures (Fig. 2-B, Supplementary Video 1). Based on the obtained results, we decided to further investigate the roles of kinin receptors in U87-MSC interactions. In this regard, visible cell fusion was observed between U87 and MSCs after 8 h of co-culture in the presence of HOE-140 and R715 (Fig. 2-C, Supplementary Video 2). MSC internalization into the U87 cell (entosis) was visualized by live-cell imaging utilizing red (U87^{DsRed}) and green-fluorescent (MSC loaded with DiO green) markers for distinct cell types and further confirmed by tracking the nucleus of the host cell in the presence of HOE-140 and R715 (Fig. 2-D, Supplementary Video 2). The nucleus acquired a moon-like shape during cell internalization and was afterward relocated during vacuole formation. Moreover, cell motility was measured by monitoring cell angulations (Supplementary Video 1 and 2). The cell directionality histograms indicate that antagonism of both kinin receptors by HOE-140 and R715 reduced cell motility of both cell types (Supplementary Video 2), reflected by reduction in the number of cells that move to different angulations (Fig. 2-E, right). These results strongly suggest that U87 cells and MSC motility was mediated by B1R and B2R activity. Observed events represent evidence of tight communication and possible crosstalk between U87 cells and MSCs *in vitro* and kininergic signaling involvement in cell motility.

Supplementary videos related to this article can be found at https://doi.org/10.1016/j.adcanc.2022.100045

3.3. Kinin-induced effects on F-actin and CD105 expression

To further investigate the relevance of pharmacological kinin receptor modulation in U87 cell and MSC interactions, we evaluated F-actin expression after treatment with BK, HOE-140 and HOE-140 plus R715 (Fig. 3-A). Application of BK did not increase the expression of F-actin in U87 cells, whereas HOE-140 decreased F-actin expression relative to BK treatment. Similarly, in U87/MSC co-culture, BK treatment did not change F-actin expression; however, HOE-140 plus R715 treatment significantly decreased F-actin expression relative to control and BK treatments, whereas HOE-140 alone also decreased its expression relative to BK treatment (Fig. 3-B). While in monoculture only 27% of U87 cells expressed F-actin, the amount of F-actin staining in U87 increased by 2-3-fold in U87 cell/MSC co-cultures after 3 days vs. control (Fig. 3C).

Based on previous findings that U87 cells acquire the MES phenotype upon co-culturing with MSCs, as judged by enhanced CD29, CD90 and CD105 expression [15], we sought to identify whether B1R and B2R activity would play a role in EMT. For this, MSC (loaded with DiO green) and U87^{DsRed} cells were co-cultured upon kinin receptor activity modulation. The cells were labeled with the anti-CD105 antibody and analyzed by flow cytometry (Fig. 3D–H). DBK treatment slightly increased the percentage of CD105-positive U87^{DsRed} cells upon co-culture (Fig. 3-F). As expected, and previously described [15], hybrid cells highly expressed CD105; however, the treatments did not alter CD105 expression (Fig. 3-G). U87 cells were selected on the fourth day from co-cultures using geneticin. BK and DBK treatments slightly increased CD105 expression in selected U87 cells (Fig. 3-H). Additionally, selected U87 cells treated with HOE-140 alone or together with R715 exhibited a slight decrease in the CD105-positive cells population (Fig. 3-H).

These results demonstrate that B1R and B2R partially modulated F-actin expression of GB cells, especially when U87 cells had been co-cultured with MSCs. Our data suggest that activities of kinin receptors, predominantly through B1R actions, promoted the transition of U87 cells towards the MES phenotype upon co-culturing with MSCs, as monitored by CD105 expression levels.

3.4. Effects of kinins on invasion and EMT gene expression in U87 cells and U87/MSC co-cultures

We hypothesized that BK might enhance U87 cell invasion. U87 and U87/MSC spheroids were treated with BK or HOE-140. BK increased the invasive potential of U87 cells and even more after one week of co-culture with MSCs (Fig. 4-A, B). B2R inhibition by HOE-140 reduced invasion compared to the control group and around 40% in comparsion to the BK treatment group in U87 monocultures (Fig. 4-B).

To reveal whether B1R and B2R activaty modulation played a role in EMT genes induction, we treated U87 monocultures and co-cultures with BK, HOE-140 or HOE-140 plus R715, thereafter selecting the U87 cells from the co-culture using geneticin, thus eliminating MSCs. On the fourth day, the surviving cells were collected for mRNA extraction and EMT gene expression analysis by real time PCR. Application of BK induced B2R, vimentin, CD44, Snail, and TGF-β gene expression in U87 cells as well as in U87 cells selected from co-culture, while this effect was hindered by HOE-140 treatment alone and HOE-140 co-treatment with

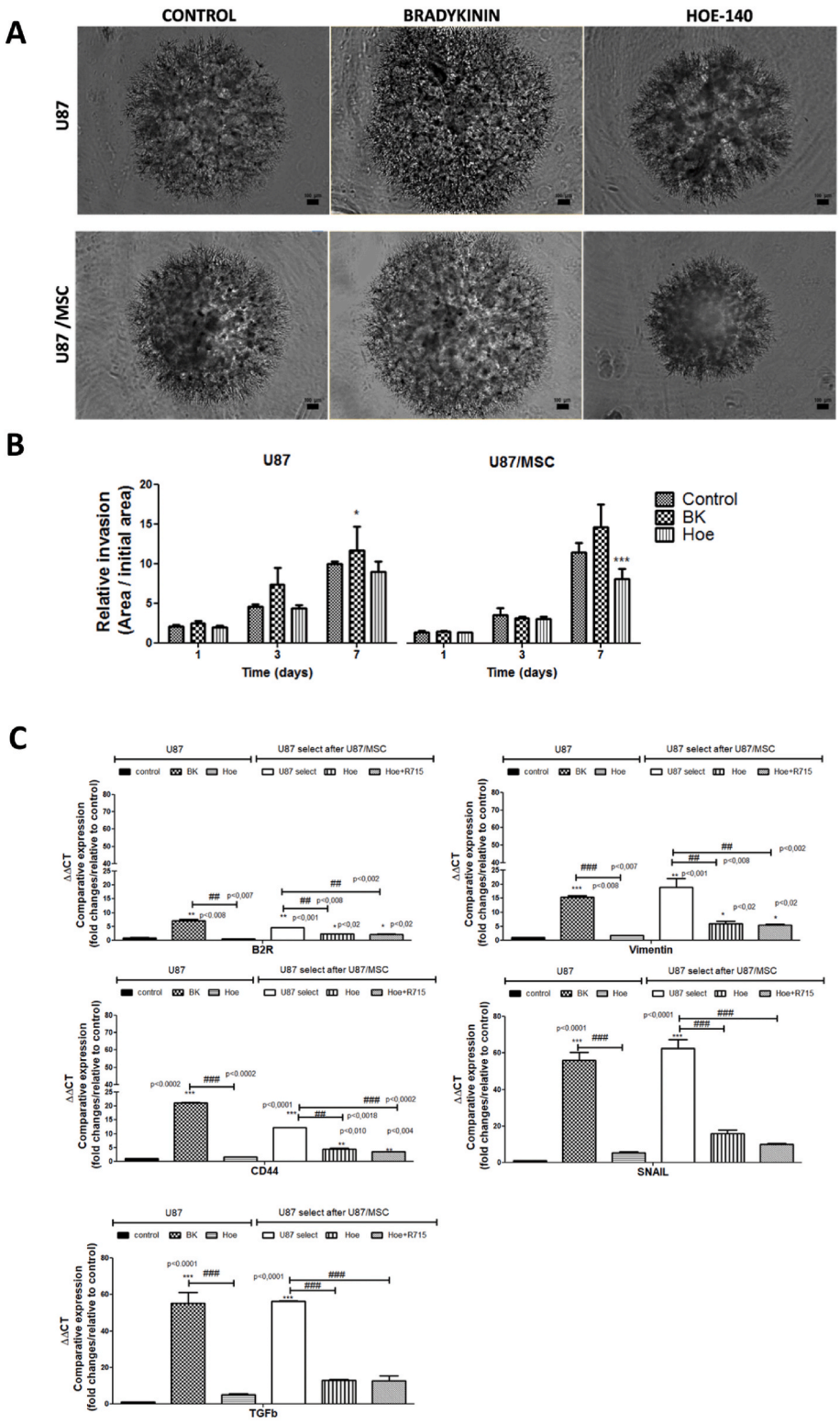

Fig. 4. Effects of kinin receptors modulation on invasion and expression levels of EMT-associated genes in U87 cells in mono- and co-cultures with MSCs. Spheroids were prepared either from U87 cells alone or U87/MSCs in a 1:1 ratio and embedded in Matrigel and imaged after 1, 3 and 7 days of culturing. **(A)** Representative images were taken following 7 days of co-culture. Scale bar = 100 μm. **(B)** Invasion (%) was determined as the ratio of the invasion area vs initial spheroid area. The two-way analysis was performed with the Bonferroni's multiple comparison test. P-value * < 0.05; *** < 0.0001. Data are representative of three independent experiments. At least 20 individual spheroids were analyzed in each experiment. **(C)** Total RNA was isolated from U87 cell monoculture and geneticin-selected U87 cells in the absence or presence of BK, HOE-140, or HOE-140 plus R715. Relative quantification of gene expression levels of B2R, Vimentin, CD44, Snail, TGF-β were normalized using GADPH, whose expression levels did not change under the used experimental conditions. Results are representative of two independent experiments with each of them performed in triplicate.

R175 (Fig. 4-C). Collectively, these results show that BK triggered the EMT gene expression and invasion of U87 cells under both mono- and co-culture conditions with MSCs.

4. Discussion

A vast body of literature reports that kininergic signaling plays a significant role in the cancer environment, including the GB microenvironment [29,39]. It is known, that both, B2R and B1R are expressed in GB cells, particularly in the PN subtype line U87, and both kinin receptors are constitutively expressed in MSCs [40,43–45]. Importantly, the expression of B1R and B2R in MSCs *in vitro* is altered in GB cells [15]. Our current investigation focused on the GB cell–MSC crosstalk mediated mainly by B2R signaling. BK treatment resulted in increased metabolic activity, suggestive of cell proliferation, of U87 and U373 cells in monocultures, but not in co-cultures with MSCs (Fig. 1).

Our data supplements the results published by Lu et al. (2010), demonstrating that upon receptor binding of DBK and BK, proliferation of GB cells increased [46]. Similar findings were reported for U138 and U251 cells, where proliferation was attributed to the activation of PI3K/Akt and ERK1/2 pathways [43]. ERK1/2 activation by BK was also reported by our group in neural progenitor (aplastic) cells [47]. The reduced sensitivity of co-cultures to kinins observed in this study may be due to a lower availability of kinin receptors or a possible induction of drug-resistance mechanisms such as gp180/MDR drug reporter protein activation upon co-culturing [48]. Additionally, MSC-GB cell crosstalk affects a plethora of intracellular signaling pathways and may be involved in the downregulation of kinin receptor activity and/or expression.

The observed co-stimulation of B1R and B2R may not be due to their direct interactions, but rather to the rapid extracellular enzymatic transformation of BK into DBK by carboxypeptidase, as reported for prostate cancer [49]. Direct proof of the importance of the interaction between these two receptors in GB was the observed inhibition of GB cell invasion following co-treatments with HOE-140 and R715. By the same token, B2R activation promoted chemotaxis and tumor invasion. We demonstrated that enhanced GB invasion by B2R signaling involved the induction of EMT-associated genes. Interestingly, the B1R receptor agonist DBK induced a slight increase in CD105 protein expression in U87-MSC co-culture and selected U87 cells, while BK had no effect in this regard. In contrast, BK induced overexpression of TGF-β in U87-MSC co-cultures. CD105 is a downstream target of the TGF-β pathway, and the observed roles for B1R and B2R suggest interferences at different levels in EMT induction. In agreement with Bryukhovetskiy and Shevchenko (2016) [54], we also observed that TGF-β expression is triggered in U87 cells by BK, while EMT-associated genes expression was prevented by these antagonists. MSC co-culture in the absence of kinin receptor agonists was sufficient to enhance the invasion of MES GB-subtype U373 cells, which express very low levels of kinin receptors, but at the same time express TGF-β [5]. Presumably, these effects were triggered by MSC-secreted or transduced factors through extracellular vesicles to make tumor cells more invasive. In contrast, the induced invasiveness of U87/MSC mixed spheroids appeared to be delayed for 4–7 days, coinciding with the appearance of heterotypic fusion events. Taken together, these data suggest selective roles of kinin receptors in neural/PN vs MES GB subtype interactions with MSCs. In the GB microenvironment *in vivo*, inflammatory cytokines may enhance kinin production and thereby augment neural/PN GB invasion. By the same token, kinin receptor antagonists may be beneficial for the individualized treatment of patients with these GB subtypes.

As reported by Fischer and coworkers (2015), within an epithelial metastatic lung tumor, only a small proportion of tumor cells undergo EMT. The authors have shown that lung metastasis mainly consist of cells that maintain their epithelial phenotype or they undergo reverse EMT transition [55]. In any case, EMT-induced migration phenotype is associated with reversible cellular morphology [56]. However, we have shown that upon B1R activation, along with invasion and EMT transition, changes in cell adherence [15] and cytoskeletal rearrangements occur. Cellular morphology and adhesion alterations are associated with highly upregulated levels of F-actin in U87/MSCs co-culture stimulated by BK, whereas F-actin expression was decreased in the presence of B1R and B2R antagonists. F-actin bundling is crucial for lamellipodia formation on the periphery of the cell. Lamellipodia is the most prominent cytoskeletal structure, that drives cell locomotion [57]. It is known that GB cell invasion is associated with cell extension of invadopodia/lamellipodia, or microspikes [53,54]. Thus, our data align with previous reports on BK as an important mediator of fibroblast motility and microspike formation [60]. Induction of F-actin expression was shown to be reduced in MSCs [61]. Cytosolic F-actin or microfilaments exhibit fast polymerization and depolymerization dynamics after co-culture treatment with BK. We observed that in most cells F-actin filaments formed larger networks that are essential for other cellular processes besides cell motility, such as vesicle and organelle movement and establishment and maintenance of cell junctions. These processes require extensive interactions of actin with cellular membranes, where kinin receptors are localized. In addition to invasion, we have also reported heterotypic cell fusion and the formation of U87:MSC hybrids that appeared within 3 days of co-culture [15,37] similar to observations made by Mercapide and coworkers (2012) [62]. Further, the fusion process was initiated by increased appearance of adherence junctions, as described for U87/MSC by Oliveira et al. (2018) [15]. Heterotypic cell fusion also occurred via U87 cells engulfing MSCs. Recently, entosis, or "cell cannibalism", of MSCs was observed in 3D co-cultures of breast cancer cells with MSCs [63]. According to Bartosh et al. (2015), MSCs can be mobilized from the bone marrow and migrate into the tumor environment [63]. Notably, MSCs are cannibalized by cancer cells, entering dormancy that suppressed their tumorigenicity. This provides a valuable tool to further understand the antitumor activity of MSCs and cell cannibalism, therefore, opens new therapeutic avenues for the prevention of cancer recurrence. Furthermore, cell fusion of MSCs with tumor cells may augment the release of pro-inflammatory molecules and a plethora of secreted cytokines, which may induce expression of the B1R [63]. Whether kinin receptors might contribute to the GB metastasis *in vivo*, as already suggested by Lah et al., 2020, needs yet to be determined [8]. Interestingly, BK has been shown to promote neuroblastoma metastasis in a mouse model [64]. This may possibly also occur in GB invasion, but needs to be explored in future.

5. Conclusions

We have shown kininergic signaling effects on cellular interactions between U87/MSCs. In direct co-cultures, U87 cells interacted with MSCs by vesicle exchange. Following treatment with B1R and B2R antagonists, cells fused, forming hetero-hybrid cells. BK treatment increased invasion of U87 cells alone and in co-cultures as well as induced overexpression of genes associated with EMT. B1R- and B2R-mediated pathways are associated with TGF-β signaling, which is an important EMT trigger. The presented data suggest the involvement of B1R and B2R in GB invasion and EMT induction with possible translational applications. *In vivo* experiments will be necessary to confirm kinin receptor functions in EMT induction.

Contributions

HU, TLL and MNO designed the research; MNO and MMP performed the experiments; HU, TLL, MNO, JB, RA wrote the manuscript; MNO, MMP, RA analyzed the data; and SLC, BLS revised the manuscript. All authors read and approved the final manuscript.

Ethics declarations

Ethics approval and consent to participate.
N/A.

Consent for publication

Obtained.

Declaration of competing interest

The authors declare that they have no known competing financial interests or personal relationships that could have appeared to influence the work reported in this paper.

Acknowledgments

This study was financed by an ARRS grant (Project J1–02474; awarded to TTL) in Slovenia; the National Council for Scientific and

Technological Development (CNPq, Linha 2 – Bolsa Pesquisador Visitante Especial [Proc. No. 402468/2012–0]) in Brazil; the São Paulo Research Foundation (FAPESP, [Proc. No. 2012/50880–4 and 2018/07366–4], granted to HU) in Brazil. TTL was a Visiting Professor within the Science without Borders Programme of the CNPq [Proc. No. 402468/2012–0]. MMP acknowledges grant support by the Research Support Foundation of the State of Rio Grande do Sul (FAPERGS, Proc. No. 21/2551-0001982-4) and a Marylou Ingram Scholarship from International Society for Advancement of Cytometry (ISAC) MO was the recipient of a CNPq doctorate fellowship in Brazil and a sandwich doctorate fellowship to perform part of her Ph.D. at the National Institute of Biology in Ljubljana, Slovenia, and was Ph.D. student at the Jožef Stefan International Postgraduate School, Ljubljana, Slovenia. The CNPq is acknowledged for researcher fellowships awarded to HU and SLC in Brazil [Proc. No. 306392/2017–8 and 307539/2018–0, respectively]. RA is recipient of a doctorate fellowship from FAPESP [Proc. No. 2019/24553–5]. JB is supported by a doctorate fellowship from Coordination for the Improvement of Higher Education Personnel (CAPES, - Finance Code 001, Brazil).

References

[1] D.N. Louis, A. Perry, G. Reifenberger, A. von Deimling, D. Figarella-Branger, W. K. Cavenee, et al., The 2016 world Health organization classification of tumors of the central nervous system: a summary, Acta Neuropathol. 131 (2016) 803–820.
[2] M. Weller, M. van den Bent, M. Preusser, E. le Rhun, J.C. Tonn, G. Minniti, et al., EANO guidelines on the diagnosis and treatment of diffuse gliomas of adulthood, Nat. Rev. Clin. Oncol. 18 (2020) 170–186.
[3] R.G.W. Verhaak, K.A. Hoadley, E. Purdom, V. Wang, Y. Qi, M.D. Wilkerson, et al., Integrated genomic analysis identifies clinically relevant subtypes of glioblastoma characterized by abnormalities in PDGFRA, IDH1, EGFR, and NF1, Cancer Cell 17 (2010) 98–110.
[4] Q. Wang, B. Hu, X. Hu, H. Kim, M. Squatrito, L. Scarpace, et al., Tumor evolution of glioma-intrinsic gene expression subtypes associates with immunological changes in the microenvironment, Cancer Cell 32 (2017) 42–56, e6.
[5] B. Breznik, H. Motaln, M. Vittori, A. Rotter, T. Lah Turnšek, Mesenchymal stem cells differentially affect the invasion of distinct glioblastoma cell lines, Oncotarget 8 (15) (2017), 2017.
[6] H. Zarkoob, J.H. Taube, S.K. Singh, S.A. Mani, M. Kohandel, Investigating the link between molecular subtypes of glioblastoma, epithelial-mesenchymal transition, and CD133 cell surface protein, PLoS One 8 (2013).
[7] B. Majc, T. Sever, M. Zarić, B. Breznik, B. Turk, T.T. Lah, Epithelial-to-mesenchymal transition as the driver of changing carcinoma and glioblastoma microenvironment, Biochim. Biophys. Acta Mol. Cell Res. 1867 (2020), 118782.
[8] T.T. Lah, M. Novak, B. Breznik, Brain malignancies: glioblastoma and brain metastases, Semin. Cancer Biol. 60 (2020) 262–273.
[9] D.F. Quail, J.A. Joyce, The microenvironmental landscape of brain tumors, Cancer Cell 31 (2017) 326–341.
[10] H. Zarkoob, J.H. Taube, S.K. Singh, S.A. Mani, M. Kohandel, Investigating the link between molecular subtypes of glioblastoma, epithelial-mesenchymal transition, and CD133 cell surface protein, PLoS One 8 (2013), e64169.
[11] C. Melzer, Y. Yang, R. Hass, Interaction of MSC with tumor cells, Cell Commun. Signal. 14 (2016) 20.
[12] J. Vieira de Castro, E.D. Gomes, S. Granja, S.I. Anjo, F. Baltazar, B. Manadas, et al., Impact of mesenchymal stem cells' secretome on glioblastoma pathophysiology, J. Transl. Med. 15 (2017) 200.
[13] F. Appaix, M.-F. Nissou, B. van der Sanden, M. Dreyfus, F. Berger, J.-P. Issartel, et al., Brain mesenchymal stem cells: the other stem cells of the brain? World J. Stem Cell. 6 (2014) 134–143.
[14] C. Schichor, V. Albrecht, B. Korte, A. Buchner, R. Riesenberg, J. Mysliwietz, et al., Mesenchymal stem cells and glioma cells form a structural as well as a functional syncytium in vitro, Exp. Neurol. 234 (2012) 208–219.
[15] M.N. Oliveira, M.M. Pillat, H. Motaln, H. Ulrich, T.T. Lah, Kinin-B1 receptor stimulation promotes invasion and is involved in cell-cell interaction of Co-cultured glioblastoma and mesenchymal stem cells, Sci. Rep. 8 (2018) 1299.
[16] N.A. Dallas, S. Samuel, L. Xia, F. Fan, M.J. Gray, S.J. Lim, et al., Endoglin (CD105): a marker of tumor vasculature and potential target for therapy, Clin. Cancer Res. 14 (2008) 1931–1937.
[17] H. Takigawa, Y. Kitadai, K. Shinagawa, R. Yuge, Y. Higashi, S. Tanaka, et al., Mesenchymal stem cells induce epithelial to mesenchymal transition in colon cancer cells through direct cell-to-cell contact, Neoplasia 19 (2017) 429–438.
[18] H. Motaln, K. Gruden, M. Hren, C. Schichor, M. Primon, A. Rotter, et al., Human mesenchymal stem cells exploit the immune response mediating chemokines to impact the phenotype of glioblastoma, Cell Transplant. 21 (2012) 1529–1545.
[19] H. Motaln, T. Turnsek, Cytokines play a key role in communication between mesenchymal stem cells and brain cancer cells, Protein Pept. Lett. 22 (2015) 322–331.
[20] S.R. Baglio, D.M. Pegtel, N. Baldini, Mesenchymal stem cell secreted vesicles provide novel opportunities in (stem) cell-free therapy, Front. Physiol. 3 (2012) 359.
[21] A. del Fattore, R. Luciano, R. Saracino, G. Battafarano, C. Rizzo, L. Pascucci, et al., Differential effects of extracellular vesicles secreted by mesenchymal stem cells from different sources on glioblastoma cells, Expet Opin. Biol. Ther. 15 (2015) 495–504.
[22] A.K. Santos, K.N. Gomes, R.C. Parreira, S. Scalzo, M.C.X. Pinto, H.C. Santiago, et al., Mouse neural stem cell differentiation and human adipose mesenchymal stem cell transdifferentiation into neuron- and oligodendrocyte-like cells with myelination potential, Stem Cell Rev. Rep. 2021 (November 15, 2021), https://doi.org/10.1007/s12015-021-10218-7.
[23] H.C. Campos, D.E. Ribeiro, D. Hashiguchi, D.Y. Hukuda, C. Gimenes, S.A. A. Romariz, et al., Distinct effects of the hippocampal transplantation of neural and mesenchymal stem cells in a transgenic model of alzheimer's disease, Stem Cell Rev. Rep. 2022 (2022), https://doi.org/10.1007/s12015-021-10321-9.
[24] C.A. Trujillo, P.D. Negraes, T.T. Schwindt, C. Lameu, C. Carromeu, A.R. Muotri, et al., Kinin-B2 receptor activity determines the differentiation fate of neural stem cells, J. Biol. Chem. 287 (2012) 44046–44061.
[25] J.M. Alves, A.H. Martins, C. Lameu, T. Glaser, N.M. Boukli, V. Bassaneze, et al., Kinin-B2 receptor activity in skeletal muscle regeneration and myoblast differentiation, Stem Cell Rev. Rep. 15 (2019) 48–58.
[26] E. Kashuba, J. Bailey, D. Allsup, L. Cawkwell, The kinin–kallikrein system: physiological roles, pathophysiology and its relationship to cancer biomarkers, Biomarkers 18 (2013) 279–296.
[27] M. Uchida, Z. Chen, Y. Liu, K.L. Black, Overexpression of bradykinin type 2 receptors on glioma cells enhances bradykinin-mediated blood–brain tumor barrier permeability increase, Neurol. Res. 24 (2002) 739–746.
[28] S. Seifert, H. Sontheimer, Bradykinin enhances invasion of malignant glioma into the brain parenchyma by inducing cells to undergo amoeboid migration, J. Physiol. 592 (2014) 5109–5127.
[29] M.M. Pillat, Á. Oliveira-Giacomelli, M. das Neves Oliveira, R. Andrejew, N. Turrini, J. Baranova, et al., Mesenchymal stem cell-glioblastoma interactions mediated via kinin receptors unveiled by cytometry, Cytometry 99 (2021) 152–163.
[30] M. Maurer, M. Bader, M. Bas, F. Bossi, M. Cicardi, M. Cugno, et al., New topics in bradykinin research, Allergy 66 (2011) 1397–1406.
[31] X. Zhang, J.L. Lowry, V. Brovkovych, R.A. Skidgel, Characterization of dual agonists for kinin B1 and B2 receptors and their biased activation of B2 receptors, Cell. Signal. 24 (2012) 1619–1631.
[32] N. Tidjane, A. Hachem, Y. Zaid, Y. Merhi, L. Gaboury, J.-P. Girolami, et al., A primary role for kinin B1 receptor in inflammation, organ damage, and lethal thrombosis in a rat model of septic shock in diabetes, Eur. J. Inflamm. 13 (2015) 40–52.
[33] F. Marceau, H. Bachelard, J. Bouthillier, J.-P. Fortin, G. Morissette, M.-T. Bawolak, et al., Bradykinin receptors: agonists, antagonists, expression, signaling, and adaptation to sustained stimulation, Int. Immunopharm. 82 (2020), 106305.
[34] E.T. Whalley, C.D. Figueroa, L. Gera, K.D. Bhoola, Discovery and therapeutic potential of kinin receptor antagonists, Expet Opin. Drug Discov. 7 (2012) 1129–1148.
[35] P. Dillenburg-Pilla, A.G. Maria, R.I. Reis, E.M. Floriano, C.D. Pereira, F.L. de Lucca, et al., Activation of the kinin B1 receptor attenuates melanoma tumor growth and metastasis, PLoS One 8 (2013) e64453–e64453.
[36] L. Molina, C.E. Matus, A. Astroza, F. Pavicic, E. Tapia, C. Toledo, et al., Stimulation of the bradykinin B1 receptor induces the proliferation of estrogen-sensitive breast cancer cells and activates the ERK1/2 signaling pathway, Breast Cancer Res. Treat. 118 (2009) 499.
[37] N.F. Nicoletti, J. Sénécal, V.D. da Silva, M.R. Roxo, N.P. Ferreira, R.L.T. de Morais, et al., Primary role for kinin B1 and B2 receptors in glioma proliferation, Mol. Neurobiol. 54 (2017) 7869–7882.
[38] V. Montana, H. Sontheimer, Bradykinin promotes the chemotactic invasion of primary brain tumors, J. Neurosci. 31 (2011) 4858–4867.
[39] M.N. Oliveira, B. Breznik, M.M. Pillat, R.L. Pereira, H. Ulrich, T.T. Lah, Kinins in glioblastoma microenvironment, Cancer Microenviron. 12 (2019) 77–94.
[40] Y.-S. Liu, J.-W. Hsu, H.-Y. Lin, S.-W. Lai, B.-R. Huang, C.-F. Tsai, et al., Bradykinin B1 receptor contributes to interleukin-8 production and glioblastoma migration through interaction of STAT3 and SP-1, Neuropharmacology 144 (2019) 143–154.
[41] M.M. Pillat, M.N. Oliveira, H. Motaln, B. Breznik, T. Glaser, T.T. Lah, et al., Glioblastoma-mesenchymal stem cell communication modulates expression patterns of kinin receptors: possible involvement of bradykinin in information flow, Cytometry 89 (2016) 365–375.
[42] A. Torsvik, G v Røsland, A. Svendsen, A. Molven, H. Immervoll, E. McCormack, et al., Spontaneous malignant transformation of human mesenchymal stem cells reflects cross-contamination: putting the research field on track – letter, Cancer Res. 70 (2010) 6393. LP – 6396.
[43] N.F. Nicoletti, T.C. Erig, R.F. Zanin, T.C.B. Pereira, M.R. Bogo, M.M. Campos, et al., Mechanisms involved in kinin-induced glioma cells proliferation: the role of ERK1/2 and PI3K/Akt pathways, J. Neuro Oncol. 120 (2014) 235–244.
[44] A.A. Nery, R.L. Pereira, V. Bassaneze, I.C. Nascimento, L.S. Sherman, P. Rameshwar, et al., Combination of chemical and neurotrophin stimulation modulates neurotransmitter receptor expression and activity in transdifferentiating human adipose stromal cells, Stem Cell Rev. Rep. 15 (2019) 851–863.
[45] M.N. Oliveira, B. Breznik, M.M. Pillat, R.L. Pereira, H. Ulrich, T.T. Lah, Kinins in glioblastoma microenvironment, Cancer Microenviron. 12 (2019) 77–94.
[46] D.-Y. Lu, Y.-M. Leung, S.-M. Huang, K.-L. Wong, Bradykinin-induced cell migration and COX-2 production mediated by the bradykinin B1 receptor in glioma cells, J. Cell. Biochem. 110 (2010) 141–150.

[47] M.M. Pillat, C. Lameu, C.A. Trujillo, T. Glaser, A.R. Cappellari, P.D. Negraes, et al., Bradykinin promotes neuron-generating division of neural progenitor cells through ERK activation, J. Cell Sci. 129 (2016) 3437–3448.
[48] D. Antoni, H. Burckel, E. Josset, G. Noel, Three-dimensional cell culture: a breakthrough in vivo, Int. J. Mol. Sci. 16 (2015).
[49] L. Barki-Harrington, A.L. Bookout, G. Wang, M.E. Lamb, L.M.F. Leeb-Lundberg, Y. Daaka, Requirement for direct cross-talk between B1 and B2 kinin receptors for the proliferation of androgen-insensitive prostate cancer PC3 cells, Biochem. J. 371 (2003) 581–587.
[53] Y. Iwadate, Epithelial-mesenchymal transition in glioblastoma progression, Oncol. Lett. 11 (2016) 1615–1620.
[54] I. Bryukhovetskiy, V. Shevchenko, Molecular mechanisms of the effect of TGF-β1 on U87 human glioblastoma cells, Oncol. Lett. 12 (2016) 1581–1590.
[55] K.R. Fischer, A. Durrans, S. Lee, J. Sheng, F. Li, S.T.C. Wong, et al., Epithelial-to-mesenchymal transition is not required for lung metastasis but contributes to chemoresistance, Nature 527 (2015) 472–476.
[56] B. Majc, M. Novak, N.K. Jerala, A. Jewett, B. Breznik, Immunotherapy of glioblastoma: current strategies and challenges in tumor model development, Cells 10 (2021) 265.
[57] H.E. Johnson, S.J. King, S.B. Asokan, J.D. Rotty, J.E. Bear, J.M. Haugh, F-actin bundles direct the initiation and orientation of lamellipodia through adhesion-based signaling, J. Cell Biol. 208 (2015) 443–455.
[60] R. Kozma, S. Ahmed, A. Best, L. Lim, The Ras-related protein Cdc42Hs and bradykinin promote formation of peripheral actin microspikes and filopodia in Swiss 3T3 fibroblasts, Mol. Cell Biol. 15 (1995) 1942–1952.
[61] Y.M. Kim, E.S. Jeon, M.R. Kim, J.S. Lee, J.H. Kim, Bradykinin-induced expression of α-smooth muscle actin in human mesenchymal stem cells, Cell. Signal. 20 (2008) 1882–1889.
[62] J. Mercapide, G. Rappa, A. Lorico, The intrinsic fusogenicity of glioma cells as a factor of transformation and progression in the tumor microenvironment, Int. J. Cancer 131 (2012) 334–343.
[63] T.J. Bartosh, M. Ullah, S. Zeitouni, J. Beaver, D.J. Prockop, Cancer cells enter dormancy after cannibalizing mesenchymal stem/stromal cells (MSCs), Proc. Natl. Acad. Sci. Unit. States Am. (2016), 201612290.
[64] H. Ulrich, M.Z. Ratajczak, G. Schneider, E. Adinolfi, E. Orioli, E.G. Ferrazoli, et al., Kinin and purine signaling contributes to neuroblastoma metastasis, Front. Pharmacol. 9 (2018) 500.